BIOCHEMISTRY
including biophysical chemistry & molecular biology

Article

pubs.acs.org/biochemistry

A Novel Form of Bacterial Resistance to the Action of Eukaryotic Host Defense Peptides, the Use of a Lipid Receptor

Sarah R. Dennison,[§] Frederick Harris,[†] Manuela Mura,[‡] Leslie H. G. Morton,[†] Andrei Zvelindovsky,[‡] and David A. Phoenix*[,§]

[§]School of Pharmacy and Biomedical Sciences, [†]School of Forensic and Investigative Sciences, and [‡]School of Computing, Engineering and Physical Sciences, University of Central Lancashire, Preston, PR1 2HE, U.K.

ABSTRACT: Host defense peptides show great potential for development as new antimicrobial agents with novel mechanisms of action. However, a small number of resistance mechanisms to their action are known, and here, we report a novel bacterial resistance mechanism mediated by a lipid receptor. Maximin H5 from *Bombina maxima* bound anionic and zwitterionic membranes with low affinity (K_d > 225 μM) while showing a strong ability to lyse (>55%) and penetrate (π > 6.0 mN m^{-1}) these membranes. However, the peptide bound *Escherichia coli* and 1,2-dimyristoyl-*sn*-glycero-3-phosphoethanolamine (DMPE) membranes with higher affinity (K_d < 65 μM) and showed a very low ability for bilayer lysis (<8%) and partitioning (π > 1.0 mN m^{-1}). Increasing levels of membrane DMPE correlated with enhanced binding by the peptide (R^2 = 0.96) but inversely correlated with its lytic ability (R^2 = 0.98). Taken with molecular dynamic simulations, these results suggest that maximin H5 possesses membranolytic activity, primarily involving bilayer insertion of its strongly hydrophobic N-terminal region. However, this region was predicted to form multiple hydrogen bonds with phosphate and ammonium groups within PE head-groups, which in concert with charge−charge interactions anchor the peptide to the surface of *E. coli* membranes, inhibiting its membranolytic action.

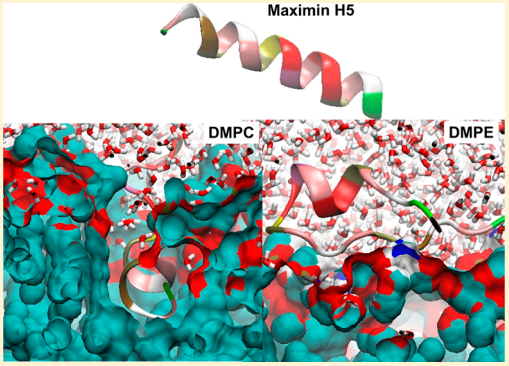

The "Golden Age of Antibiotics" began in the 1940s with the introduction of penicillin,[1] and in 1967, it was stated by the U.S. surgeon William H. Stewart that "..we had essentially defeated infectious diseases and could close the book on them..".[2] Instead, the latter decades of the 20th century and the first decade of the 21st century were notable for the appearance of pathogenic bacteria with resistance to conventional antibiotics as an almost inevitable response to the introduction of these drugs into clinical medicine.[1] The rapid rise of these multidrug resistant (MDR) pathogens[3] is well-illustrated by *Escherichia coli*, which remains a global cause of morbidity and mortality.[4] *E. coli* is normally a commensal organism of the gastrointestinal tract, but a number of recent surveys have shown that pathogenic strains of the organism with MDR increased from below 8% during the 1950s to approaching 65% in the 2000s with the occurrence of these MDR strains consistently highest for antimicrobial agents that had been used the longest in human and veterinary medicine.[5,6] Currently, MDR forms of the organism are a leading cause of nosocomial infections[7,8] and have been responsible for recent major community outbreaks of infectious diseases, including the potentially fatal condition hemolytic-uremic syndrome.[9,10] On the basis of the relative ease and adaptability with which *E. coli* acquires resistance to antibiotics, along with its common occurrence across many different species, the organism is now used as a sentinel to monitor the development of antimicrobial drug resistance in other bacterial pathogens.[11]

Unchecked, the current upward trend in the occurrence of pathogenic bacteria with MDR creates the very real threat that in a short while there will be no suitable antimicrobials for the systemic treatment of common diseases.[12] Accordingly, there have been concerted attempts to identify alternative strategies for the control of bacterial infections,[13,14] including the development of host defense peptides (HDPs), which are ancient and highly effective antimicrobials of the innate immune system.[15,16] The antibacterial activity of these peptides involves multiple sites of action rather than the individual gene and protein targets associated with the action of conventional antibiotics. Moreover, evidence suggests that HDPs target membrane integrity, bioenergetics, and other essential systems of bacteria that are less mutable than the bacterial targets of conventional antibiotics. On the basis of these observations, it is generally believed that the emergence of bacteria with resistance to the action of HDPs is less likely, thereby helping to explain their longevity and potentially giving them a major therapeutic advantage over conventional antibiotics.[15,17−19] Nonetheless, bacterial resistance mechanisms to the action of HDPs, such as the production of both intracellular and extracellular proteases to effect degradation of these peptides,[20,21] have been reported. Many of these resistance

Received: June 7, 2013
Revised: July 26, 2013
Published: July 29, 2013

   dx.doi.org/10.1021/bi400719j | *Biochemistry* 2013, 52, 6021−6029

mechanisms have been identified in *E. coli*[20,21] with the result that the organism has been increasingly used to monitor and study the development of bacterial resistance to HDPs.[22−24] The present study reports a novel resistance mechanism to the action of HDPs against *E. coli* and shows that intrinsic properties of the organism's membrane allow a mode of antibacterial action used by these peptides to be harnessed as a mechanism of resistance to their activity. Phosphatidylethanolamine (PE) is a major lipid in the membranes of *E. coli*[25] that has been shown to act as a lipid receptor for several HDPs and promote their action against the organism.[26] However, in contrast, our data show that PE acts as an inhibitor of maximin H5 activity, an anionic HDP recently identified in the skin and brain of the Chinese red belly toad, *Bombina maxima*.[27,28]

EXPERIMENTAL PROCEDURES

Materials. A peptide homologue of maximin H5 was synthesized by Pepceuticals (Leicestershire, UK) by solid state synthesis and purified by HPLC to a purity greater than 99%. The lipids, *E. coli* cardiolipin (CA), 1,2-dimyristoyl-*sn*-glycero-3-phosphocholine (DMPC), 1,2-dimyristoyl-*sn*-glycero-3-phosphoglycerol (DMPG), 1,2-dimyristoyl-*sn*-glycero-3-phosphoethanolamine (DMPE), and the lipid probe, fluorescein-phosphatidylethanolamine (FPE), were supplied by Avanti Polar Lipids (USA). Unless otherwise stated, all other reagents were supplied by Sigma-Aldrich (UK) and VWR (UK).

Molecular Dynamic Simulations of Maximin H5−Membrane Interactions. Molecular dynamic (MD) simulations to model the interactions of maximin H5 with DMPC and DMPE membranes were undertaken. The peptide was assembled using the AMBER tools 1.5 program[29] and minimized using the GROMOS96 53a6 force field,[30] which was equilibrated at room temperature in water. These bilayers contained 128 lipids in a box, which was 7.0 nm × 7.0 nm × 9.0 nm in the case of DMPC and 5.6 nm × 5.6 nm × 9 nm in the case of DMPE, parallel to the *z*-axis. The GROMOS96 force field step descendent method was utilized to minimize the structure and, employing a 400 ns equilibration run at 303 K (∼30 °C), simulations were performed using the NPT ensemble. Three peptide molecules were inserted into the box containing the solvated bilayer, and an equilibration run was carried out for the system. The stability of maximin H5 association with the surface of DMPE bilayers was estimated by determining the energy required to force the peptide to occupy a location in the membrane interior, which was performed using the potential of mean force (PMF) facility available in Gromacs.[31] The potential energy of the system was extracted for the slower pulling simulations with a pulling rate of 0.1 Å/ns for 40 ns. The peptide was pulled in the direction parallel to the *Z* axis.[31]

The Antibacterial Activity of Maximin H5. Cultures of *E. coli*, strain W3110, and *Staphylococcus aureus*, strain UL12, which had been freeze-dried in 20% (v/v) glycerol and stored at −80 °C, were used to inoculate 10 mL aliquots of sterile Nutrient broth and incubated at 37 °C until the exponential phase was reached (OD = 0.6; λ = 600 nm). Using a benchtop centrifuge, the cell suspension was centrifuged at 15000*g* and 4 °C for 10 min. The resulting pellet was washed three times in 25% strength Ringer's solution before being resuspended in 25% strength Ringer's solution. One milliliter aliquots of maximin H5 ranging from 0 μM to 1000 μM were prepared in 25% strength Ringer's solution. These peptide solutions were inoculated with 10 μL cell suspensions and incubated at 37 °C overnight. After incubation, each bacterial culture was streaked onto nutrient agar plates and incubated at 37 °C for 12 h.

The Preparation of Small Unilamellar Vesicles. Small unilamellar vesicles (SUVs) were constructed with a mean diameter of 0.1 μM as previously described.[32] Essentially, either prelipids or lipid mixtures were dissolved in chloroform (5 mg mL^{-1}), dried under N_2, and further dried under vacuum overnight. The resulting lipid film was rehydrated using phosphate buffered saline (PBS; pH 7.5) containing NaCl (150 mM) and sonicated for an hour or until the solution was no longer turbid. To form SUVs, these solutions were then freeze−thawed (×5) and extruded (×11) using an Avanti polar lipid mini-extruder apparatus containing a 0.1 μm polycarbonate filter (Avanti, USA).

CD Structural Analyses of Maximin H5. Structural determination of maximin H5 was performed using CD spectroscopy and a J-815 spectropolarimeter (JASCO, UK) as previously described. Far-UV CD spectra were collated for peptide (0.1 mg mL^{-1}) both in PBS and in the presence of SUVs prepared as described above from either CA, DMPG, DMPC, DMPE or mixtures of CA, DMPG, and DMPE (molar ratio 2:1:13.7) mimetic of *E. coli* membranes.[25] For each sample, four scans were performed over a wavelength range 260 to 180 nm at 0.5 nm intervals using a bandwidth of 1 nm and a scan speed of 100 nm min^{-1}. CD spectra were measured using a 10 mm path-length cell, and samples were maintained at 20 °C. For all spectra acquired, the baseline obtained in the absence of peptide was subtracted, all as previously described.[33] These experiments were repeated four times, and the average percentage of secondary structural elements was estimated for peptides using the CDSSTR method (protein reference set 3) from the DichroWeb server.[34,35]

Interaction of Maximin H5 with Lipid Monolayers. Either CA, DMPG, DMPE, DMPC mixtures of DMPG and DMPE (molar ratio varying between 10:1 and 200:1) or mixtures of CA, DMPG, and DMPE (molar ratio 2:1:13.7) mimetic of *E. coli* membranes[25] were taken and dissolved in a minimum of chloroform. Monolayers were formed by dropping these chloroformic solutions onto a buffer subphase (Tris10 mM; pH 7.5), contained in a 601 M Langmuir Trough equipped with moveable barriers (KVS NIMA, UK). The barriers were closed at a rate of 5 cm^2 min^{-1} until an initial surface pressure of 30 mN m^{-1} was achieved, which is generally taken as representative of naturally occurring membranes, and then monolayers were allowed to equilibrate for 30 min. Using an L-shaped Hamilton syringe, maximin H5 (1 mM) was injected into the subphase to give a final subphase concentration of 8 μM, which was continuously mixed with a magnetic stirrer at 5 rpm, and changes in surface pressure (π) were measured using the Wilhelmy plate method, all as previously described.[33] These experiments were repeated four times, and the maximum change in surface pressure was averaged.

Binding of SUVs by Maximin H5. SUVs were prepared as described above from either DMPG, DMPE, mixtures of DMPG and DMPE (molar ratio varying between 10:1 and 200:1), or mixtures of CA, DMPG, and DMPE (molar ratio 2:1:13.7) mimetic of *E. coli* membranes[25] except that 0.5 mol % of FPE was added to the organic solvent before drying. After drying, the resulting lipid films were hydrated with Tris-HCl (10 mM; pH 7.4) containing EDTA (1 mM) to give a final lipid concentration of 10 mg mL^{-1}. SUVs were diluted to 65 μM, and fluorescence was recorded using an FP-6500

spectrofluorometer (JASCO, UK) with an excitation wavelength of 492 nm and an emission wavelength of 516 nm: the excitation and emission slits were set to 5 nm. The incorporation of FPE label into SUVs was verified as previously described[32] by observing fluorescence changes when SUVs were incubated with (i) Ca^{2+} (10 mM) and (ii) calcimycin (3.0 μM), a calcium ionophore (A23187). To investigate the binding of maximin H5 to FPE-labeled SUVs, the peptide was added to these lipid bodies to give final concentrations in the range 0−250 μM and fluorescence monitored. Changes in the fluorescence (ΔF) of FPE-labeled SUVs induced by the addition of maximin H5 were then plotted as a function of peptide concentration and fitted by nonlinear least-squares analysis to the equation below where [M] is the concentration of maximin H5, F_{max} is the maximum fluorescence change and K_d is the binding coefficient of the peptide.[32]

$$\Delta F = \frac{\Delta F_{max}[M]}{K_d + [M]} \quad (1)$$

To gain insight into the binding of maximin H5 to *E. coli* membranes, the change in fluorescence intensity observed upon the addition of the peptide (100 μM) to FPE labeled SUVs, which were mimetic of *E. coli* membranes (CA/DMPG/DMPE, molar ratio 2:1:13.7[25]) was recorded. The effects on fluorescence induced by the subsequent addition of Ca^{2+} and calcimycin were also recorded. Similar analyses were performed using maximin H5 (200 μM) and FPE labeled SUVs formed from either: DMPG, DMPE, or mixtures of these lipids (DMPG/DMPE molar ratio varying between 10:1 and 200:1) to gain a better understanding of the role of PE in the binding of the peptide to *E. coli* membranes.

Lysis of SUVs by Maximin H5. SUVs were prepared as described above from either DMPG, DMPE, mixtures of DMPG and DMPE (molar ratio varying between 10:1 and 20:1), or mixtures of CA, DMPG, and DMPE (molar ratio 2:1:13.7) mimetic of *E. coli* membranes[25] except that lipid (7.5 mg) was dissolved in chloroform. After drying, the resulting lipid film was hydrated with 1 mL of HEPES (5 mM; pH 7.5) containing calcein (70 mM). SUVs with entrapped calcein were separated from free calcein by gel filtration using HEPES (5 mM; pH 7.5) as an elutant and a Sephadex G75 column (Sigma-Aldrich, UK), which was hydrated overnight with HEPES (20 mM; pH 7.4) containing NaCl (150 mM) and EDTA (1.0 mM). The ability of maximin H5 to lyse these SUVs was determined by assaying calcein release. Aliquots (20 μL) of solutions containing SUVs with entrapped calcein and maximin H5 at final concentrations in the range 0 μM to 400 μM were incubated with 2 mL of HEPES (20 mM; pH 7.4) containing NaCl (150 mM) and EDTA (1.0 mM). The fluorescence intensity of released calcein was measured using an FP-6500 spectrofluorometer (JASCO, UK) with an excitation wavelength of 490 nm and an emission wavelength of 520 nm. The change in fluorescence observed for calcein release when SUVs were dissolved in Triton-X100 (20 μL) was taken to represent 100% lysis and used to determine the percentage lysis of these SUVs by maximin H5. These experiments were repeated four times and the percentage lysis was averaged.

RESULTS

Antibacterial Assay of Maximin H5. Cultures of *E. coli*, strain W3110, were incubated with maximin H5, and it was found that this strain was strongly resistant to the action of the peptide up to maximin H5 concentrations of 1000 μM. In contrast, *S. aureus*, strain UL12 was highly susceptible to the action of maximin H5, which showed a minimum inhibitory concentration (MIC) of 90 μM, in agreement with previously published results.[28]

Molecular Dynamic (MD) Simulations of Maximin H5−Membrane Interactions. MD simulations to model interactions between maximin H5 and either DMPC or DMPE membranes were undertaken (Figures 1, 2, and 3). These simulations predicted that in the presence of membranes formed from either DMPE or DMPC, the peptide would adopt molecular architectures with levels of α-helicity of 55% and 40% respectively. These simulations also predicted that maximin H5 would interact with these membranes via differing modes of action, involving a variety of hydrogen bonds and charge−charge associations (Figures 1, 2, and 3).

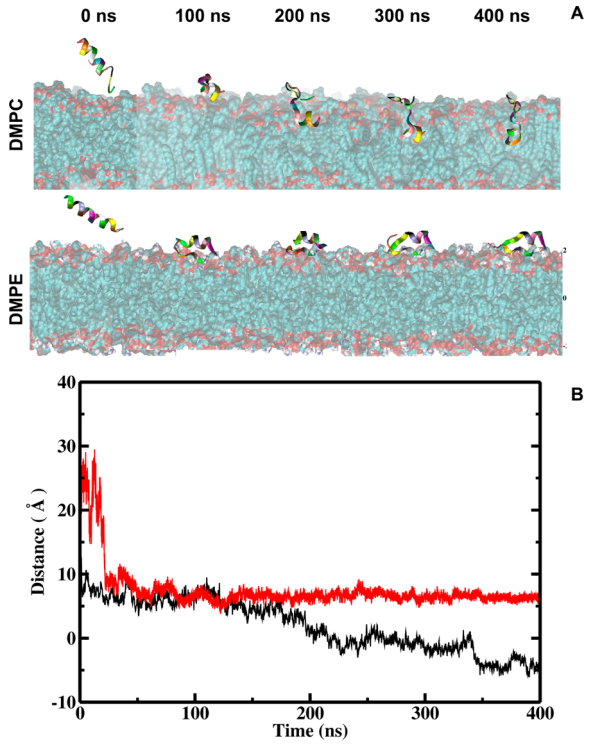

Figure 1. Molecular dynamic simulation of maximin H5. Panel A shows snapshots at fixed time points highlighting the interaction between maximin H5 and lipid bilayers formed from either DMPC or DMPE. Panel B shows the distance between the center of mass of the peptide and center of lipid bilayer DMPC (in black) and DMPE (in red) with time.

In the case of DMPC, maximin H5 took ca. 100 ns to attain the membrane interface, and after 200 ns, the peptide interacted with the hydrophobic core of the bilayer. After 300 ns, maximin H5 clearly inserted deeper into the central region of the DMPC bilayer, and at the end of the 400 ns simulation the peptide was predominantly located in the membrane interior in an orientation perpendicular to the bilayer surface (Figures 1A and 2A). To measure the depth of penetration shown by maximin H5 in DMPC membranes, the distance between the center of mass of the peptide and the top of PO_4 groups in the DMPC bilayer was plotted for the course of the simulation (Figure 1B). This distance increased over the course of MD simulations in the direction of the membrane core and

dx.doi.org/10.1021/bi400719j | *Biochemistry* 2013, 52, 6021−6029

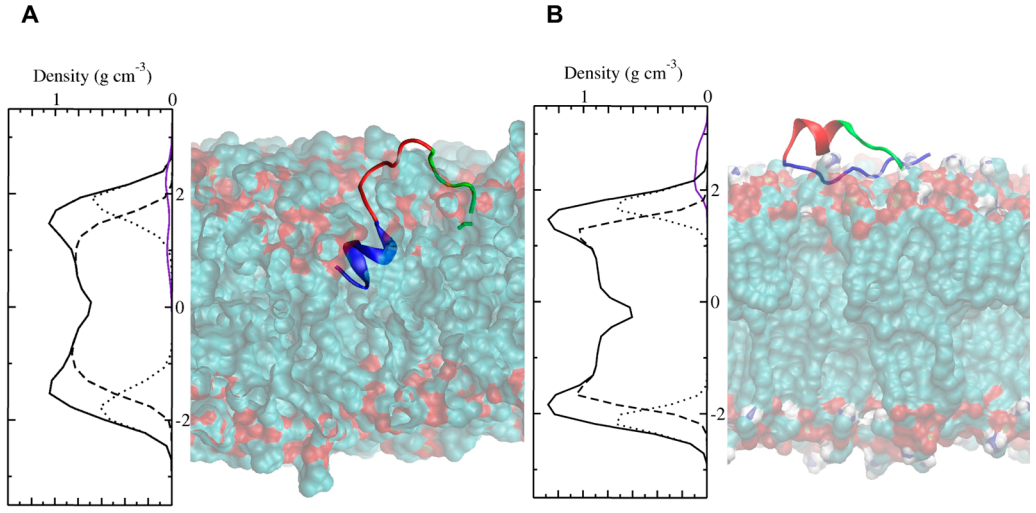

Figure 2. The final molecular dynamic snapshot configuration of maximin H5−membrane interactions. Maximin H5 with DMPC bilayer (A) and maximin H5 with DMPE bilayer (B). In each figure, the right-hand image is a simulation snapshot after 400 ns, The peptide coloring follows this scheme: the hydrophobic N-terminal region (H_2N-ILGPVLGLVS) is shown in blue, the aspartic acid-rich segment (DTLDD) is shown in red, and the C-terminal residues (VLGIL-NH_2) are depicted in green. Left-hand graphics in each panel shows partial densities of the components: overall lipid density (solid black line), lipid head-groups (dots), lipid tails groups (dashed line), and peptide (purple line).

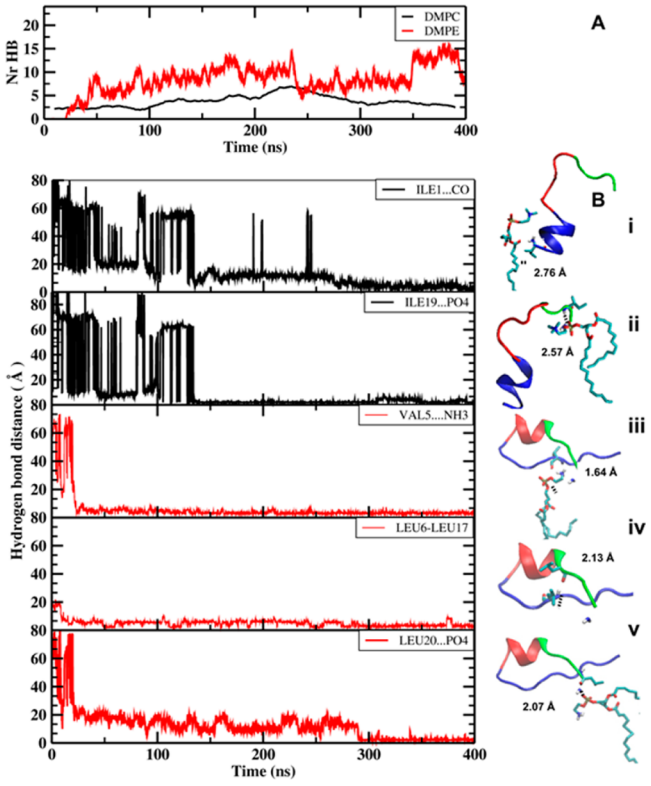

Figure 3. Molecular dynamic analysis of hydrogen bonding. (A) The number of hydrogen bonds (NrHB) as a function of time in the presence of DMPC (black) and DMPE (red). (B) The plots show examples the time evolution of hydrogen bond formation between maximum H5 the lipid bilayer DMPE (red) and DMPC (black) over the course of the simulation. The right-hand side illustrates the distance between the relevant groups at the end of the simulation after 400 ns (i−v).

predicted that the peptide would insert into the DMPC bilayer to a depth of around 5 Å or 0.5 nm, after 400 ns, indicating deep penetration into the bilayer consistent with membranolytic activity (Figure 1B).

In the case of DMPE, maximin H5 reached the membrane interface after 100 ns. After 300 ns, the peptide lay parallel to the membrane surface, remaining in this orientation until the end of the simulation at 400 ns (Figures 1A and 2B). To measure the depth of penetration shown by maximin H5 in DMPE membranes, the distance between the center of mass of the peptide and the top of PO_4 groups in the DMPC bilayer was again plotted for the course of the simulation (Figure 1B). After 30 ns, this distance remained constant for the duration of the 400 ns simulation at 0.5 nm above the membrane surface, indicating that maximin H5 has no substantial propensity to partition into the DMPE bilayer (Figure 1B).

The evolution of hydrogen bond formation for the interaction of H5 interaction with membranes formed from either DMPC or DMPE was modeled using MD simulations (Figure 3A). At the end of the 400 ns simulation, three hydrogen bonds were observed between maximin H5 and the DMPC bilayer, which involved the CO and PO_4 groups of the lipid head-group region (Figure 3A). Ile1 of maximin H5 formed two hydrogen bonds with DMPC membranes, which involved the amide moiety of the residue and the CO group of the lipid. The initial distance between head-group and peptide molecule was 80 Å and decreased to 5 Å after 130 ns as the hydrogen bond was formed. At the end of the 400 ns, simulation bond lengths were 2.76 Å, indicating the creation of a moderate hydrogen bond (Figure 3B (i)). Similar behavior was observed for Ile19 of maximin H5, which showed that the NH group on the backbone of the residue hydrogen bonded to the PO_4 moiety of DMPC. In this case, the initial distance was 90 Å, which was reduced to 2.5 Å after 140 ns indicating strong hydrogen bonds and remained so for the duration of the simulation (Figure 3B (ii)). The amide moiety located on Leu20 of maximin H5 also formed hydrogen bonds with CO groups of the DMPC bilayer, and, in addition, there was a hydrogen bond between the NH group of the backbone of this residue and the PO_4 moiety of DMPC (data not shown).

In the case of DMPE, a total of eight hydrogen bonds were observed between maximin H5 and the lipid bilayer at the end of MD simulations. These hydrogen bonds involved the PO_4

dx.doi.org/10.1021/bi400719j | *Biochemistry* 2013, 52, 6021−6029

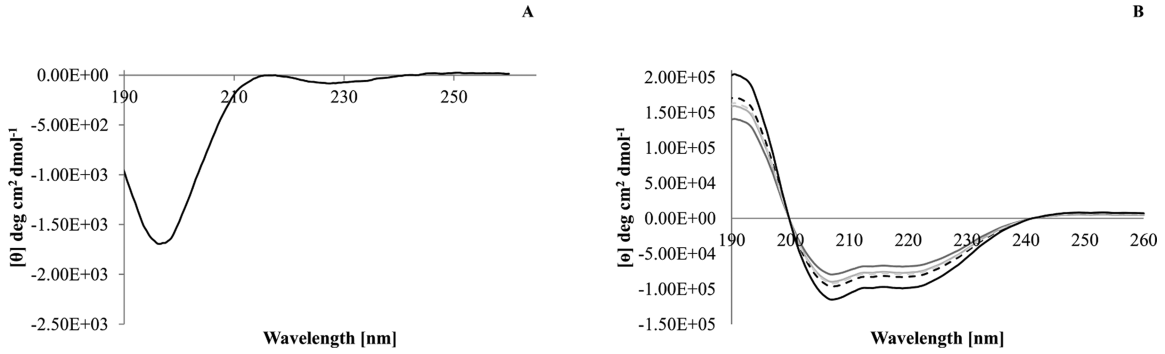

Figure 4. CD structural analyses of maximin H5. Figure shows representative structural analyses of maximin H5. In panel A, the aqueous peptide was mainly formed from β-type structures (50%; Table 1). Panel B shows that maximin H5 adopted predominantly α-helical architecture in the presence of SUVs formed from CA (solid gray), DMPE (solid black), DMPC (solid light gray), DMPG (solid light gray dotted), and lipids derived from *E. coli* (dotted black). These levels of α-helicity ranged from 40 to 61% (Table 1).

and NH_3 groups of the lipid head-group region with examples shown in Figure 3. Val5 of the peptide formed hydrogen bonds with the NH_3 and CO groups of DMPE where the initial hydrogen bond distance was 75 Å. This distance decreased to 7 Å after 30 ns and reduced to 3 Å the end of the simulation (Figure 3B (iii)). In addition, in this conformation an intrapeptide hydrogen bond was predicted for maximin H5, which involved the NH group on the backbone of Leu6 and the CO moiety of Leu17. The initial distance for this hydrogen bond was 25 Å, which was reduced to 3 Å at the end of the simulation (Figure 3B (iv)). The amide moiety of the peptide's Leu20 formed two hydrogen bonds with the PO_4 groups of the DMPE bilayer with an the initial distance of 75 Å, which was decreased to 25 Å at 20 ns and reduced to 2 Å at the end of the simulation as the hydrogen bond formed (Figure 3B (v)). Other hydrogen bonds predicted for the interaction of maximin H5 and with DMPE bilayers followed the same general trend in formation as those of residues illustrated in Figure 3B (iv and v). These interactions primarily involved NH_3 and PO_4 groups of DMPE and Ile1, Pro4, Leu6, Gly7, Leu8, and Ser10 of maximin H5 (data not shown).

CD Structural Analysis of Maximin H5. CD analysis was used to study the conformational behavior of maximin H5. In aqueous solution, the peptide was predominantly formed from β-strands and turns (50%) with the remainder mainly showing an unordered structure (Figure 4; Table 1). In the presence of pure anionic lipids (CA and DMPG), pure zwitterionic lipids (DMPC and DMPE) and lipid mixtures mimetic of *E. coli* membranes (CA/DMPG/DMPE, molar ratio 2:1:13.7[25]), the peptide underwent conformational change and adopted a predominantly α-helical structure, which ranged from 40 to 61% (Figure 4; Table 1). The levels of this secondary structure were significantly higher ($F_{5,23}$ = 8096.49; p = 0.00) for maximin H5 in the presence of DMPE (61%) as compared to those of other lipids (<50%).

Interaction of Maximin H5 with Lipid Monolayers. The ability of maximin H5 to partition into a variety of lipid monolayers was investigated (Table 2) with representative examples of these interactions shown in Figure 5. The peptide was found to strongly partition into monolayers formed from the anionic lipids CA and DMPG, inducing surface pressure changes of 6.4 and 9.0 mN m^{-1} respectively (Figure 5, Table 2). The peptide showed a variable ability to partition into zwitterionic lipid monolayers, inducing the highest surface pressure change observed with DMPC (π = 11 mN m^{-1}), but showed no ability to partition into DMPE (π = 0.01 mN m^{-1})

Table 1. Effect of Lipid on Secondary Structural Contributions to Maximin H5[a]

maximin H5	% α-helix	% β-strand	% β-turns	% unordered
aqueous solution	2.0 ± 0.7	27.0 ± 0.7	23.0 ± 0.7	48.0 ± 1.4
DMPG	46.0 ± 0.7	19.0 ± 0.7	16.0 ± 0.7	19.0 ± 2.1
DMPE	61.0 ± 1.5	15.0 ± 1.0	8.0 ± 1.5	16.0 ± 1.0
DMPC	43.0 ± 0.0	27.0 ± 2.1	9.0 ± 0.7	22.0 ± 2.1
CA	40.0 ± 1.2	31.0 ± 2.5	7.0 ± 2.0	22.0 ± 1.5
E. coli membrane mimics	47.0 ± 1.5	25.0 ± 1.0	7.0 ± 2.0	21.0 ± 1.5

[a]The structural contributions to the molecular architecture of maximin H5 in aqueous solution and in the presence of SUVs formed from a range of anionic and zwitterionic lipids. SUVs mimetic of *E. coli* membranes were formed from CA, DMPG, and DMPE at a molar ratio of 2:1:13.7. These data show that in the presence of both anionic and zwitterionic lipid, maximin H5 adopts a predominantly α-helical structure. The levels of this secondary structure were significantly higher ($F_{5,23}$ = 8096.49; p = 0.00) for maximin H5 in the presence of DMPE (61%) as compared to those of other lipids (<50%).

monolayers (Figure 5, Table 2). Maximin H5 also showed only a very limited propensity (π = 0.9 mN m^{-1}) to partition into monolayers formed from lipid mixtures mimetic of *E. coli* membranes (CA/DMPG/DMPE molar ratio 2:1:13.7[25]) (Figure 5, Table 2). In the case of monolayers formed from mixtures of DMPG and DMPE, the highest surface pressure change observed for these monolayers was 6.3 mN m^{-1} at a DMPG/DMPE ratio of 200:1, while the lowest was 2.0 mN m^{-1} at a DMPG/DMPE ratio of 10:1 (Table 2). These data showed that maximin H5 had a generally high ability to partition into both anionic and zwitterionic membranes, other than those formed from phosphatidylethanolamine (PE), with a strong inverse correlation between the levels of PE present in the monolayer and the ability of the peptide to partition (R^2 = 0.96).

Binding and Lysis of SUVs by Maximin H5. The ability of maximin H5 to bind and lyse a variety of lipid SUVs was investigated (Table 2). The peptide bound to vesicles formed from DMPC with a K_d of 245 μM and DMPG with a K_d of 230 μM while showing a strong ability to lyse these lipid bodies (57.5% and 61.6% respectively). However, maximin H5 bound SUVs formed from either DMPE or lipid mixtures mimetic of *E. coli* membranes (CA/DMPG/DMPE molar ratio 2:1:13.7[25]) with an affinity that was ca. 5-fold higher (K_d = 55 and 65 μM respectively, Table 2) and showed only a weak ability to lyse

dx.doi.org/10.1021/bi400719j | *Biochemistry* 2013, 52, 6021−6029

Table 2. Effect of Lipid Composition on the Membrane Interactions of Maximin H5[a]

lipids	monolayer π (mN m^{-1})	binding to SUVs K_d (μM)	lysis of SUVs calcein release (%)
CA	6.0 ± 0.24		
DMPC	11.0 ± 0.42	245.1 ± 3.10	61.6 ± 2.26
DMPG	9.4 ± 0.51	229.9 ± 0.65	57.5 ± 2.58
DMPG/DMPE 200:1	6.3 ± 0.42	211.7 ± 1.98	42.9 ± 2.20
DMPG/DMPE 100:1	5.1 ± 0.21	196.5 ± 1.98	38.7 ± 2.26
DMPG/DMPE 50:1	3.7 ± 0.14	178.9 ± 1.90	32.5 ± 1.94
DMPG/DMPE 20:1	2.7 ± 0.20	149.9 ± 0.61	19.2 ± 0.82
DMPG/DMPE 10:1	2.0 ± 0.14	95.8 ± 0.73	11.2 ± 2.21
DMPE	0.01 ± 0.03	54.4 ± 2.79	5.3 ± 2.65
E. coli membrane mimics	0.9 ± 0.21	65.0 ± 1.40	7.6 ± 0.14

[a]The interaction of maximin H5 (including standard deviations) with anionic lipids, zwitterionic lipids and mixtures of these lipids presented in various systems. The partitioning of the peptide into monolayers formed from these lipids was determined as the maximum pressure change induced (π mN m^{-1}). The affinity of maximin H5 for SUVs formed from these lipids was measured as its binding coefficient (K_d), and the ability of the peptide to lyse these lipid bodies was quantified by the percentage of calcein released by its lytic action. Monolayers and SUVs mimetic *E. coli* membranes were formed from CA, DMPG, and DMPE at a molar ratio of 2:1:13.7. These data showed that maximin H5 had a generally high ability to lyse and penetrate both anionic and zwitterionic membranes, which correlated inversely with PE levels in these membranes ($R^2 > 0.9$ in all cases). Conversely, these data also showed that the ability of the peptide to bind to these membranes correlated directly with their DMPE levels ($R^2 = 0.98$).

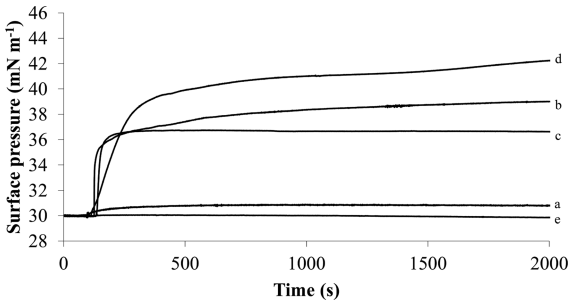

Figure 5. The interaction of maximin H5 with lipid monolayers. Figure shows surface pressure changes induced by the partitioning of maximin H5 into monolayers formed from (a) lipid mixtures mimetic of *E. coli* membranes (CA/DMPG/DMPE molar ratio 2:1:13.7), (b) DMPG, (c) CA, (d) DMPC, and (e) DMPE. The maximum surface pressure changes observed in these monolayer interactions (π mN m^{-1}) were derived and are shown in Table 2.

these vesicles (5.3% in the case of DMPE and 7.6% in the case of *E. coli* membrane mimics; Table 2). In the case of SUVs formed from mixtures of DMPG and DMPE, at low DMPE levels (DMPG/DMPE ≥ 100:1), the peptide bound these vesicles with K_d values that were >200 μM and achieved levels of membrane lysis that were >35%. At high DMPE levels (DMPG/DMPE ≤ 20:1), the peptide bound these vesicles with K_d values that were <150 μM and exhibited levels of membrane lysis that were <20% (Table 2). These data showed that the level of DMPE in membranes correlated directly with the ability of maximin H5 to bind to these lipid bodies ($R^2 = 0.96$) and inversely with the peptide's ability to cause lysis ($R^2 = 0.98$).

DISCUSSION

It is well established that PE serves as a membrane receptor in promoting the toxicity of a number of prokaryotic HDPs toward bacteria and eukaryotic cells.[36] There is also accumulating evidence that the lipid may serve a similar role in the activity of some eukaryotic HDPs as recently proposed for human Aβ40 and Aβ42, which appear to possess amyloid-mediated antimicrobial properties.[37,38] Currently, the major focus of research into the role of PE-binding in the defense function of HDPs is cyclotides from plants,[26,39,40] some of which utilize the lipid to promote their action against a range of bacteria including *E. coli*.[41−43] However, in contrast to this emerging role for PE-binding by HDPs to increase efficacy, here, we show that the intrinsic properties of *E. coli* membranes have allowed the organism to harness the affinity of PE for these peptides to mediate its resistance to the action of maximin H5 from *B. maxima*.[27,28]

Our biophysical studies showed that maximin H5 possessed a generally strong ability to lyse and partition into both anionic and zwitterionic membranes other than those inclusive of PE where this ability was reduced in a manner that correlated closely with levels of the lipid present ($R^2 > 0.95$; Table 2). Taken with the fact that PE forms ca. 80% of the lipid in the *E. coli* inner membrane,[25] these data suggested that this lipid may play a role in the resistance of the organism to the action of maximin H5. Consistent with this suggestion, the peptide was found to have an affinity for DMPE and *E. coli* membranes that was ca. 5-fold higher than that of other lipid membranes (Table 2) and was comparable to those of several PE-binding cyclotides.[42,43] These peptides possess affinities for PE that are in the low micromolar range and, similarly to maximin H5, are anionic and ineffective against Gram-negative bacteria. However, the mechanisms underpinning this bacterial resistance have not, as yet, been definitively elucidated.[42,43]

To gain insight into the affinity of maximin H5 for PE, molecular dynamic simulations were undertaken, which predicted that the peptide would reside on the surface of DMPE membranes, primarily *via* associations involving the N-terminal region of the peptide (Figures 1A and 2B). This region was predicted to possess random coil structure and was therefore flexible, which allows the formation of a hydrogen bonding network with phosphate and ammonium groups within the DMPE head-group region (Figure 3B (iv and v)). Bordering on this N-terminal region was a peptide segment rich in aspartic acid residues, which was strongly α-helical and included the bulk of the structure predicted for maximin H5 in the presence of DMPE (Figures 1A and 2B). This α-helical segment appeared to serve a structural role by promoting a bend in the chain of the peptide, which then formed a bridge over the PE-binding sequence of maximin H5 and terminated by forming multiple hydrogen bonds with moieties in the DMPE head-group region (Figures 2B and 3B (iv)). This overall conformation stabilized the peptide/membrane interface and overcame an energy barrier to insertion, therefore decreasing the efficiency of H5 membrane partitioning.

To confirm that the affinity of maximin H5 for PE was specific for this lipid rather than zwitterionic lipids in general, molecular dynamic simulations were used to model the interaction of the peptide with phosphatidylcholine (PC), which is present in the membranes of ca. 10% of bacteria.[44]

dx.doi.org/10.1021/bi400719j | *Biochemistry* 2013, 52, 6021−6029

These simulations predicted that maximin H5 would insert deeply into a DMPC bilayer in an almost perpendicular orientation relative to the membrane surface (Figures 1A and 2A). In this orientation, the PE-binding sequence of the peptide was located in the apolar core of the membrane and was the major site of α-helical structure predicted for maximin H5 in the presence of the lipid. As reported for other HDPs that adopt membrane interactive α-helical structure, this conformational preference is well-known to enhance the lipid interactivity of peptides by maximizing their hydrophobic surfaces.[16,17,19,33] Stabilizing these hydrophobic membrane interactions, the aspartic acid-rich segment of maximin H5 was predicted to possesses random coil structure that facilitated association with moieties in the DMPC head-group *via* multiple hydrogen bonds and charge−charge interactions (Figure 3A,B). This form of membrane penetration is typical of membranolytic HDPs[26,38,45] and may represent that generally used by maximin H5 to promote its antibacterial action, given the strongly lipid-interactive nature of the peptide (Table 2).

This study strongly reinforces the view that a complete description of the membrane interactions of HDPs can only be obtained when the characteristics of both these peptides *and* their target membranes are taken into account.[16,19] For example, PE and PC are the major zwitterionic lipids in bacterial membranes and differ only in relation to the constituents carried by the N^+ moiety in their head-groups, which are H and CH_3 respectively.[25] However, recent studies have shown that these structural differences can have a profound effect on the properties of membranes formed by PE and PC such as fluidity and lipid packing.[46] These effects were recently seen on studies on aureins, which are cationic amphibian HDPs, when these peptides were found to possess a much greater ability to insert into PC/PG bilayers as compared to those formed from PE/PG. This inhibitory effect appeared to be based on the smaller size of the PE head-group compared to that of PC, which allowed tighter lipid packing in membranes formed from PE/PG, thereby reducing the ability of aureins to partition into these bilayers.[47] In the present study, it has been suggested that the ability of anionic maximin H5 to engage in multiple interactions with PE, which are unavailable to PC and other lipids, may underpin the resistance of *E. coli* to the action of the peptide. For example, maximin H5 was predicted to form hydrogen bonds with the ethanolamine moiety of DMPE (Figure 3B), but clearly it cannot form such bonds with the choline moieties of DMPC, whose methyl groups lack this facility.[48] On the basis of our combined data, we propose a mechanism to explain the resistance of *E. coli* to the action of maximin H5. At the bacterial membrane interface, the peptide adopts an α-helical structure (Table 1), which in the case of membranes depleted in PE, leads to penetration of the bilayer core region by maximin H5 and bacterial cell death via membranolytic mechanisms. In the case of PE-rich bacterial membranes, head-group interactions stabilize the structure of the peptide by the induction of significantly higher levels of α-helical architecture, which is localized in the peptide's aspartate-rich segment (≥ca. 15%; Table 1). Concomitant with this conformational change, the peptide's N-terminal segment binds strongly to the membrane surface, thereby inhibiting bilayer penetration by this segment and promoting adoption of the bridged structure depicted in Figures 1A and 2 for maximin H5. In this orientation, membrane penetration by maximin H5 may be further inhibited by the tethering effect imparted by the presence of the bridging segment and the association of its C-terminus with the membrane. Moreover, in this orientation, the close proximity of hydrophobic residues in the PE-binding and bridging segments of the peptide (Figures 1A and 2) would help compensate for the energetically unfavorable location of these residues in the PE head-group region and its environment. In combination, the overall conformation of the peptide coupled to its ability to form multiple hydrogen bonds with the PE head-group region stabilizes the association of maximin H5 with the membrane surface. In turn, these membrane associations make the transfer of the peptide into the membrane interior energetically more expensive, which was estimated by MD simulations to be ca. 560 KJ/mol, and this energy barrier makes a major contribution to preventing the membranolytic activity of the peptide (Table 2).

In conclusion, this would appear to be the first report of a bacterial resistance mechanism to HDPs mediated by a lipid receptor, and it expands the repertoire of microbial resistance mechanisms to the action of these peptides. In addition to *E. coli*, this knowledge might also help explain the ineffectiveness of maximin H5 against a range of other microbes with PE-rich membranes, including bacteria and fungi[26,28] along with enveloped viruses.[49] Conversely, the absence of PE in the membranes of *S. aureus*[25] may help explain the susceptibility of the organism to maximin H5.[28] Although, as suggested for other anionic HDPs,[50] it is also possible that this susceptibility may involve the interaction of maximin H5 with positively charged lipids such as lysylphosphatidylglycerol, which is richly represented in the membranes of *S. aureus*.[25] Taken in combination, it is also hoped that the data presented here will help in the design of HDPs and thereby enhance the strong potential shown by these peptides to act as therapeutically useful antibacterial agents.[15,18,51]

AUTHOR INFORMATION

Corresponding Author

*Address: Prof. D. A. Phoenix, Office of the Vice Chancellor, University of Central Lancashire, Preston PR1 2HE, U.K. E-mail: daphoenix@uclan.ac.uk. Phone: +44 (0) 1772 892504. Fax: +44 (0) 1772 892936.

Funding

The authors thank the Volkswagen Foundation for the financial support (ref.: 83932).

Notes

The authors declare no competing financial interest.

ACKNOWLEDGMENTS

The authors thank HPCT at the University of Central Lancashire. The authors also thank Dr. Marco Pinna for useful discussions on the molecular dynamic simulations.

ABBREVIATIONS USED

K_d, binding coefficient; CA, *Escherichia coli*, cardiolipin; DMPC, 1,2-dimyristoyl-*sn*-glycero-3-phosphocholine; DMPE, 1,2-dimyristoyl-*sn*-glycero-3-phosphoethanolamine; DMPG, 1,2-dimyristoyl-*sn*-glycero-3-phosphoglycerol; FPE, fluorescein-phosphatidylethanolamine; HDPs, host defense peptides; MIC, minimum inhibitory concentration; MD, molecular dynamic; MDR, multidrug resistant; PBS, phosphate buffered saline; PC, phosphatidylcholine; PE, phosphatidylethanolamine; SUV, small unilamellar vesicles

REFERENCES

(1) Davies, J., and Davies, D. (2010) Origins and Evolution of Antibiotic Resistance. Microbiol. *Mol. Biol. Rev. 74*, 417−433.

(2) Spellberg, B., Guidos, R., Gilbert, D., Bradley, J., Boucher, H. W., Scheld, W. M., Bartlett, J. G., and Edwards, J. (2008) The Epidemic of Antibiotic-Resistant Infections: A Call to Action for the Medical Community from the Infectious Diseases Society of America. *Clin. Infect. Dis. 46*, 155−164.

(3) Boucher, H. W., Talbot, G. H., Bradley, J. S., Edwards, J. E., Jr., Gilbert, D., Rice, L. B., Scheld, M., Spellberg, B., and Bartlett, J. (2009) Bad Bugs, No Drugs: No ESKAPE! An Update from the Infectious Diseases Society of America. *Clin. Infect. Dis. 48*, 1−12.

(4) Da Silva, G. J., and Mendonca, N. (2012) Association between antimicrobial resistance and virulence in Escherichia coli. *Virulence 3*, 18−28.

(5) Tadesse, D. A., Zhao, S., Tong, E., Ayers, S., Singh, A., Bartholomew, M. J., and McDermott, P. F. (2012) Antimicrobial Drug Resistance in *Escherichia coli* from Humans and Food Animals, United States, 1950−2002. *Emerg. Infect. Dis. 18*, 741−749.

(6) Cullen, I. M., Manecksha, R. P., McCullagh, E., Ahmad, S., O'Kelly, F., Flynn, R. J., McDermott, T., Murphy, P., Grainger, R., Fennell, J. P., and Thornhill, J. A. (2012) The changing pattern of antimicrobial resistance within 42 033 *Escherichia coli* isolates from nosocomial, community and urology patient-specific urinary tract infections, Dublin, 1999−2009. *BJU Int. 109*, 1198−1206.

(7) Pitout, J. D. D. (2012) Extraintestinal Pathogenic *Escherichia coli*: A Combination of Virulence with Antibiotic Resistance. *Front microbiol. 3*, 1−7.

(8) Totsika, M., Moriel, D. G., Idris, A., Rogers, B. A., Wurpel, D. J., Phan, M. D., Paterson, D. L., and Schembri, M. A. (2012) Uropathogenic *Escherichia coli* Mediated Urinary Tract Infection. *Curr. Drug Targets 13*, 1386−1399.

(9) Malecki, M., Mattner, F., and Schildgen, O. (2012) Short review: molecular diagnosis of *Escherichia coli* O104:H4. *Rev. Med. Microbiol. 23*, 14−17.

(10) Pexara, A., Angelidis, D., and Govaris, A. (2012) Shiga toxin-producing *Escherichia coli* (STEC) food-borne outbreaks. *J. Hellenic. Vet. Med. Soc. 63*, 45−53.

(11) von Baum, H., and Marre, R. (2005) Antimicrobial resistance of *Escherichia coli* and therapeutic implications. *Int. J. Med. Microbiol. 295*, 503−511.

(12) Cars, O., Hedin, A., and Heddini, A. (2011) The global need for effective antibiotics-Moving towards concerted action. *Drug Resist. Updat. 14*, 68−69.

(13) Harris, F., and Pierpoint, L. (2012) Photodynamic therapy based on 5-aminolevulinic acid and its use as an antimicrobial Agent. *Med. Res. Rev. 32*, 1292−1327.

(14) Lloyd, D. H. (2012) Alternatives to conventional antimicrobial drugs: a review of future prospects. *Vet. Dermatol. 23* (299−304), e259−260.

(15) Pasupuleti, M., Schmidtchen, A., and Malmsten, M. (2012) Antimicrobial peptides: key components of the innate immune system. *Crit. Rev. Biotechnol. 32*, 143−171.

(16) Harris, F., Dennison, S. R., and Phoenix, D. A. (2009) Anionic Antimicrobial Peptides from Eukaryotic Organisms. *Curr. Protein Pept. Sci. 10*, 585−606.

(17) Harris, F., Dennison, S. R., and Phoenix, D. A. (2011) Anionic Antimicrobial Peptides from Eukaryotic Organisms and their Mechanisms of Action. *Curr. Chem. Biol. 5*, 142−153.

(18) Yount, N. Y., and Yeaman, M. R. (2012) Emerging Themes and Therapeutic Prospects for Anti-Infective Peptides. *Annu. Rev. Pharmacol. Toxicol. 52*, 337−360.

(19) Dennison, S. R., Wallace, J., Harris, F., and Phoenix, D. A. (2005) Amphiphilic alpha-helical antimicrobial peptides and their structure/function relationships. *Protein Pept. Lett. 12*, 31−39.

(20) Koprivnjak, T., and Peschel, A. (2011) Bacterial resistance mechanisms against host defense peptides. *Cell. Mol. Life Sci. 68*, 2243−2254.

(21) Gruenheid, S., and Le Moual, H. (2012) Resistance to antimicrobial peptides in Gram-negative bacteria. *FEMS Microbiol. Lett. 330*, 81−89.

(22) Maria-Neto, S., Candido, E. d. S., Rodrigues, D. R., de Sousa, D. A., da Silva, E. M., Pepe de Moraes, L. M., de Jesus Otero-Gonzalez, A., Magalhaes, B. S., Dias, S. C., and Franco, O. L. (2012) Deciphering the Magainin Resistance Process of *Escherichia coli* Strains in Light of the Cytosolic Proteome. *Antimicrob. Agents Chemother. 56*, 1714−1724.

(23) Kai-Larsen, Y., Lüthje, P., Chromek, M., Peters, V., Wang, X., Holm, Å., Kádas, L., Hedlund, K.-O., Johansson, J., Chapman, M. R., Jacobson, S. H., Römling, U., Agerberth, B., and Brauner, A. (2010) Uropathogenic *Escherichia coli* Modulates Immune Responses and Its Curli Fimbriae Interact with the Antimicrobial Peptide LL-37. *PLoS Pathog. 6*, e1001010.

(24) Radhouani, H., Pinto, L., Poeta, P., and Igrejas, G. (2012) After genomics, what proteomics tools could help us understand the antimicrobial resistance of *Escherichia coli*? *J. Proteomics 75*, 2773−2789.

(25) Lohner, K., and Prenner, E. J. (1999) Differential scanning calorimetry and X-ray diffraction studies of the specificity of the interaction of antimicrobial peptides with membrane-mimetic systems. *Biochim. Biophys. Acta 1462*, 141−156.

(26) Phoenix, D. A., Dennison, S. R., and Harris, F. (2013) Models for the membrane interactions of antimicrobial peptides. in Antimicrobial peptides (Phoenix, D. A., Dennison, S. R., and Harris, F. Eds.) pp 145−180, Wiley, Germany.

(27) Liu, R., Liu, H., Ma, Y., Wu, J., Yang, H., Ye, H., and Lai, R. (2011) There are Abundant Antimicrobial Peptides in Brains of Two Kinds of Bombina Toads. *J. Proteome Res. 10*, 1806−1815.

(28) Lai, R., Liu, H., Lee, W. H., and Zhang, Y. (2002) An anionic antimicrobial peptide from toad Bombina maxima. *Biochem. Biophys. Res. Commun. 295*, 796−799.

(29) AMBER (2010) http:/ambermd.org.

(30) Hess, B., Kutzner, C., van der Spoel, D., and Lindahl, E. (2008) GROMACS 4: Algorithms for Highly Efficient, Load-Balanced, and Scalable Molecular Simulation. *J. Chem. Theory Comput. 4*, 435−447.

(31) Lumb, C. N., He, J., Xue, Y., Stansfeld, P. J., Stahelin, R. V., Kutateladze, T. G., and Sansom, M. S. (2011) Biophysical and computational studies of membrane penetration by the GRP1 pleckstrin homology domain. *Structure 19*, 1338−1346.

(32) Wall, J., Golding, C. A., Van Veen, M., and O'Shea, P. (1995) The use of fluoresceinphosphatidylethanolamine (FPE) as a real-time probe for peptide-membrane interactions. *Mol. Membr. Biol. 12*, 183−192.

(33) Dennison, S. R., Morton, L. H. G., and Phoenix, D. A. (2012) Role of molecular architecture on the relative efficacy of aurein 2.5 and modelin 5. *Biochim. Biophys. Acta 1818*, 2094−2102.

(34) Whitmore, L., and Wallace, B. A. (2004) DICHROWEB, an online server for protein secondary structure analyses from circular dichroism spectroscopic data. *Nucleic Acids Res. 32*, W668−W673.

(35) Whitmore, L., and Wallace, B. A. (2008) Protein secondary structure analyses from circular dichroism spectroscopy: Methods and reference databases. *Biopolymers 89*, 392−400.

(36) Zhao, M. (2011) Lantibiotics as probes for phosphatidylethanolamine. *Amino Acids 41*, 1071−1079.

(37) Harris, F., Dennison, S. R., and Phoenix, D. A. (2012) Aberrant action of amyloidogenic host defense peptides: a new paradigm to investigate neurodegenerative disorders? *FASEB J. 26*, 1776−1781.

(38) Phoenix, D. A., Dennison, S. R., and Harris, F. (2013) Anionic Antimicrobial Peptides, in *Antimicrobial Peptides* (Phoenix, D. A., Dennison, S. R., and Harris, F., Eds.) pp 83−113, Wiley, Germany.

(39) Henriques, S. T., Huang, Y.-H., Rosengren, K. J., Franquelim, H. G., Carvalho, F. A., Johnson, A., Sonza, S., Tachedjian, G., Castanho, M. A. R. B., Daly, N. L., and Craik, D. J. (2011) Decoding the Membrane Activity of the Cyclotide Kalata B1. The Importance of Phosphatidiletanolamine Phospholipids and Lipid Organization on Hemolytic and anti-HIV Activities. *J. Biol. Chem. 286*, 24231−24241.

(40) Burman, R., Strömstedt, A. A., Malmsten, M., and Göransson, U. (2011) Cyclotide−membrane interactions: Defining factors of

membrane binding, depletion and disruption. *Biochim. Biophys. Acta 1808*, 2665−2673.
(41) Prabhu, S., Dennison, S., Lea, B., Snape, T., Nicholl, I., Radek, I., and Harris, F. (2013) Anionic antimicrobial and anticancer peptides from plants. *Crit. Rev. Plant Sci. 32*, 303−320.
(42) Henriques, S. T., Huang, Y.-H., Castanho, M. A. R. B., Bagatolli, L. A., Sonza, S., Tachedjian, G., Daly, N. L., and Craik, D. J. (2012) Phosphatidylethanolamine binding is a conserved feature of cyclotide-membrane interactions. *J. Biol. Chem . 287*, 33629−33643.
(43) Pranting, M., Loov, C., Burman, R., Goransson, U., and Andersson, D. I. (2010) The cyclotide cycloviolacin O2 from Viola odorata has potent bactericidal activity against Gram-negative bacteria. *J. Antimicrob. Chemother. 65*, 1964−1971.
(44) Sohlenkamp, C., López-Lara, I. M., and Geiger, O. (2003) Biosynthesis of phosphatidylcholine in bacteria. *Prog. Lipid Res. 42*, 115−162.
(45) Phoenix, D. A., Dennison, S. R., and Harris, F. (2013) Cationic antimicrobial peptides and their structure/function relationships, in *Antimicrobial Peptides* (Phoenix, D. A., Dennison, S. R., and Harris, F., Eds.) pp 39−81, Wiley, Germany.
(46) Madrid, E., and Horswell, S. L. (2013) Effect of headgroup on the physicochemical properties of phospholipid bilayers in electric fields: size matters. *Langmuir 29*, 1695−1708.
(47) Cheng, J. T., Hale, J. D., Elliott, M., Hancock, R. E., and Straus, S. K. (2011) The importance of bacterial membrane composition in the structure and function of aurein 2.2 and selected variants. *Biochim. Biophys. Acta 1808*, 622−633.
(48) Murzyn, K., Rog, T., and Pasenkiewicz-Gierula, M. (2005) Phosphatidylethanolamine-phosphatidylglycerol bilayer as a model of the inner bacterial membrane. *Biophys. J. 88*, 1091−1103.
(49) Wang, G. S., Watson, K. M., Peterkofsky, A., and Buckheit, R. W. (2010) Identification of Novel Human Immunodeficiency Virus Type 1-Inhibitory Peptides Based on the Antimicrobial Peptide Database. *Antimicrob. Agents Chemother. 54*, 1343−1346.
(50) Dennison, S. R., Morton, L. H., Brandenburg, K., Harris, F., and Phoenix, D. A. (2006) Investigations into the ability of an oblique alpha-helical template to provide the basis for design of an antimicrobial anionic amphiphilic peptide. *FEBS J. 273*, 3792−3803.
(51) Afacan, N. J., Yeung, A. T. Y., Pena, O. M., and Hancock, R. E. W. (2012) Therapeutic Potential of Host Defense Peptides in Antibiotic-resistant Infections. *Curr. Pharm. Des. 18*, 807−819.